Braz J Phys (2017) 47:321–332
DOI 10.1007/s13538-017-0499-7

GENERAL AND APPLIED PHYSICS

# Approximate Transmission Coefficients in Heavy Ion Fusion

**A. J. Toubiana[1,2] · L. F. Canto[3,4] · M. S. Hussein[5,6,7]**

Received: 15 March 2017 / Published online: 21 April 2017


**Abstract** In this paper, we revisit the one-dimensional tunneling problem. We consider different approximations for the transmission through the Coulomb barrier in heavy ion collisions at near-barrier energies. First, we discuss approximations of the barrier shape by functional forms where the transmission coefficient is known analytically. Then, we consider Kemble's approximation for the transmission coefficient. We show how this approximation can be extended to above-barrier energies by performing the analytical continuation of the radial coordinate to the complex plane. We investigate the validity of the different approximations considered in this paper by comparing their predictions for transmission coefficients and cross sections of three heavy ion systems with the corresponding quantum mechanical results.

**Keywords** Heavy ion reactions · Fusion · Quantum tunneling · Transmission coefficients

✉ M. S. Hussein
hussein@if.usp.br

A. J. Toubiana
ajtoubiana@gmail.com

L. F. Canto
canto@if.ufrj.br

[1] Departamento de Engenharia Nuclear, Escola Politécnica, Universidade Federal do Rio de Janeiro, C.P. 68529, 21941-909, Rio de Janeiro, RJ, Brazil

[2] École CentraleSupélec, Plateau de Moulon, 3 rue Joliot-Curie, 91192 Gif-sur-Yvette, France

[3] Instituto de Física, Universidade Federal do Rio de Janeiro, CP 68528, 21941-972, Rio de Janeiro, RJ, Brazil

[4] Instituto de Física, Universidade Federal Fluminense, Av. Litoranea s/n, Gragoatá, Niterói, R.J., 24210-340, Brazil

[5] Departamento de Física Matemática, Instituto de Física, Universidade de São Paulo, C.P. 66318, 05314-970, São Paulo, SP, Brazil

[6] Instituto de Estudos Avançados, Universidade de São Paulo, C.P. 72012, 05508-970, São Paulo, SP, Brazil

[7] Departamento de Física, Instituto Tecnológico de Aeronáutica, CTA, São José dos Campos, São Paulo, SP, Brazil

## 1 Introduction

The transmission through a potential barrier is a remarkable feature of quantum mechanics. Since Gamow's theory of alpha decay, in 1928, it has been used to explain a variety of new phenomena. In particular, the transmission coefficients through the Coulomb barrier have been an important ingredient in calculations of heavy ion fusion cross sections along the last few decades. In single-channel descriptions of heavy ion scattering, fusion is frequently simulated by a strong imaginary potential acting in the inner side of the Coulomb barrier. Since the fraction of the incident current that reaches the strong absorption region is fully absorbed, the fusion probability at each partial wave can be approximated by the transmission coefficient through the Coulomb + centrifugal barriers.

Although the transmission coefficients through an arbitrary potential barrier can be evaluated by numerical procedures, it is convenient to have analytical expressions. This is possible in some particular cases, like the parabolic barrier [1] and the Morse [2] barrier. In the case of alpha-decay Li et al. [3] used a different approximation for the barrier

which also resulted in an analytical form for the transmission coefficient. Parabolic barriers have been used for decades in fusion reactions of heavy ions [4–7]. In this case, the barrier at each partial wave is approximated by a parabola, with properly chosen parameters, and the transmission coefficients are given by an analytical expression involving these parameters. However, although this approximation is very good near the barrier radius, it becomes progressively worse as the radial distance increases. The reason for this shortcoming is that the parabola is symmetric around the barrier radius, whereas the actual barrier is highly asymmetric. The latter falls off very slowly at large distances (like $1/r$), while the former decreases rapidly. This exerts great influence on the transmission coefficient at energies well below the barrier, which are very sensitive to the potential at large distances. Thus, the parabolic approximation cannot be used to evaluate transmission coefficients in this energy region. The situation is better if one approximates the Coulomb barrier by a Morse function. Although it leads to a more complicated analytical expression, this barrier has the advantage of being asymmetric. Similar to the Coulomb barrier, it falls off slowly at the tail, and rapidly in the inner region.

Owing to the short wavelengths involved in heavy ion collisions, the transmission coefficients are frequently evaluated by semiclassical approximations, like the WKB (for a recent review, see Ref. [8]). However, although this approximation has been very successful at energies well below the Coulomb barrier, it fails at energies near the Coulomb barrier and above. Kemble [9] derived an improved version of the WKB approximation that remains valid at energies just below the Coulomb barrier. Further, he suggested that his expression for the transmission coefficient could be extended to energies above the barrier through an analytical continuation of the radial variable to the complex plane. In a previous work [10], we followed this procedure to study Kemble's approximation for a typical heavy ion potential, below and above the barrier. We concluded that the transmission coefficient and cross sections evaluated in this way were in good agreement with their quantum mechanical counterparts.

The present work reports a detailed study of parabolic and Morse approximations for the Coulomb + centrifugal barriers, and the resulting transmission coefficients and fusion cross sections. It investigates also the use of Kemble's approximation for the transmission coefficients through these barriers, at energies above and below the Coulomb barrier. We show that Kemble's approximation in these cases becomes exact, independently of the collision energy. The paper is organized as follows. In Section 2, we present a brief description of the single-channel approach to the fusion cross section in heavy ion scattering. In Section 3, the main section of this work, we discuss approximate calculations of transmission coefficients and fusion cross sections. We consider the approximation of the barrier by a parabola and by a Morse function, and different versions of the WKB approximation for the transmission coefficients. We discuss also the Wong formula for the fusion cross section and recent improvements to it. In Section 4, we apply the approximations of the previous section to the calculation of transmission coefficients and fusion cross sections. We consider a few light and medium mass systems, namely $^{4}$He + $^{16}$O, $^{12}$C + $^{16}$O, and $^{16}$O + $^{208}$Pb. It is expected that the accuracy of these approximations improves with the mass of the system [6]. Finally, in Section 5, we present the conclusions of the present work.

## 2 Fusion Reactions in Heavy Ion Collisions

In single-channel descriptions of heavy ion scattering, the fusion process is usually simulated by an imaginary potential. This potential is very strong and has a short range, so that it acts exclusively in the inner region of the potential barrier, resulting from nuclear attraction plus Coulomb repulsion. The scattering wave function is expanded in partial waves, leading to a radial equation for each angular momentum. The real part of the potential, appearing in the radial equations, can be written as

$$V_l(r) = V_{\rm C}(r) + V_{\rm N}(r) + \frac{\hbar^2}{2\mu\, r^2}\, l(l+1), \tag{1}$$

where the Coulomb interaction between the finite nuclei is usually approximated by the expression

$$V_{\rm C}(r) = \frac{Z_{\rm P} Z_{\rm T}\, e^2}{r}, \qquad \text{for } r \geq R_{\rm C}, \tag{2}$$

$$= \frac{Z_{\rm P} Z_{\rm T}\, e^2}{2\, R_{\rm C}} \left(3 - \frac{r^2}{R_{\rm C}^2}\right), \qquad \text{for } r < R_{\rm C}, \tag{3}$$

with

$$R_{\rm C} = r_{0\rm C} \left(A_{\rm P}^{1/3} + A_{\rm T}^{1/3}\right).$$

In the above equations, $Z_{\rm P}$ ($A_{\rm P}$) and $Z_{\rm T}$ ($A_{\rm T}$) are respectively the projectile's and target's atomic (mass) numbers, and we take $r_{0\rm C} \simeq 1$ fm.

Different procedures have been proposed to determine the nuclear interaction between two heavy ions (see, e.g. [11] and references therein). Among them, the double-folding model [12] is a systematic procedure that has the advantage of being applicable to any heavy ion system. In this model, the potential is given by a multi-dimensional integral involving the densities of the two nuclei and a realistic nucleon-nucleon interaction. On the other hand, this model has the unpleasant feature of requiring the evaluation of a rather complicate integral. To avoid this problem, Akyüz and Winther [13] proposed a simplified version of

the double-folding model. They evaluated the folding integral for a large number of systems, and fitted the resulting potential by the Woods-Saxon (WS) function,

$$V_{\rm N}(r) = \frac{V_0}{1+\exp\left[(r-R_0)/a_0\right]}, \tag{4}$$

with $R_0 = r_0\left(A_{\rm P}^{1/3}+A_{\rm T}^{1/3}\right)$. The parameters $V_0$, $r_0$, and $a_0$ were then given by analytical expressions of the mass numbers of the collision partners. This potential is adopted throughout the present work. The values of the WS parameters for the systems studied here are given in Table 1.

Usually, the loss of the incident flux to the fusion channel is simulated by a short-range imaginary potential. The radial equation is then solved numerically, starting from $r = 0$, and the elastic scattering and the fusion cross sections are determined from the $l$ components of the S-matrix, $S_l$, given by the asymptotic form of the radial wave function.

An equivalent method to simulate the fusion process is the *ingoing wave boundary condition* (IWBC). In this method, the potential is real but the integration of the radial equation does not start at the origin. It starts at some radial distance in the inner region of the barrier (usually, the minimum of the total potential), where the radial wave function is assumed to have a purely ingoing behavior. The initial values of the wave function and of its derivative are then evaluated by the WKB approximation. We adopt this procedure in the present work.

The fusion cross section is then given by the partial wave sum

$$\sigma_{\rm F} = \frac{\pi}{k^2}\sum_{l=0}^{\infty}(2l+1)\;P_l^{\rm F}, \tag{5}$$

with the fusion (absorption) probability,

$$P_l^{\rm F} = 1-|S_l|^2\,. \tag{6}$$

Since the wave function inside the barrier is totally absorbed, the fusion probability must be very close to the probability that the incident current reaches the point of total absorption. Thus, it can be approximated by the tunneling probability through the corresponding $l$-dependent barrier. That is,

$$P_l^{\rm F} \simeq T_l\,. \tag{7}$$

**Table 1** Strengths, radius parameters, and diffusivities in the Woods-Saxon parametrization of the Akyüz-Winther interaction for the systems studied in the present paper

| System | $^{4}$He + $^{16}$O | $^{12}$C + $^{16}$O | $^{16}$O + $^{208}$Pb |
|---|---|---|---|
| $V_0$ (MeV) | −29.64 | −39.47 | −64.97 |
| $r_0$ (fm) | 1.156 | 1.163 | 1.179 |
| $a_0$ (fm) | 0.5535 | 0.5928 | 0.6576 |

We use this approximation to derive the fusion cross sections from the transmission coefficients of our approximate calculations.

## 3 Approximate Transmission Coefficients and Fusion Cross Sections

Now, we discuss different approximations for the transmission coefficients mentioned in the previous section. We consider approximations of the Coulomb barrier itself and discuss the use of different versions of the WKB approximation in the calculation of transmission coefficients. We discuss also Wong's approximation for the fusion cross section, which is widely used in the study of heavy ion fusion.

### 3.1 Approximations of the Potential Barriers

The transmission coefficient for some particular barriers can be evaluated analytically. This is the case of the parabolic [1] and the Morse [2] barriers. These results can be used in calculations of fusion cross sections in heavy ion collisions. For this purpose, one approximates the potential barriers of $V_l(r)$ by parabolae or by Morse functions, with properly chosen parameters. To simplify the discussion, we consider only S-waves. Other angular momenta can be handled similarly.

#### *3.1.1 Parabolic Barrier*

Let us consider a parabolic barrier written as

$$V(r) = V_{\rm B} - \frac{1}{2}\,\mu\omega^2\;(r-R_{\rm B})^2\,. \tag{8}$$

It corresponds to an inverted harmonic oscillator with the maximum at $r = R_{\rm B}$, with the value $V(r=R_{\rm B}) = V_{\rm B}$. The barrier curvature parameter, $\hbar\omega$, is related to the second derivative of the total potential at $r = R_{\rm B}$ by the equation,

$$\hbar\omega = \sqrt{\frac{-\hbar^2\,V''(R_{\rm B})}{\mu}}.$$

The transmission coefficient through this barrier, known in the literature as the *Hill-Wheeler transmission coefficient*, can be written as

$$T_0^{\rm HW}(E) = \frac{1}{1+\exp\left[2\,\Phi^{\rm HW}(E)\right]}, \tag{9}$$

with

$$\Phi^{\rm HW}(E) = \frac{\pi}{\hbar\omega}\;(V_{\rm B}-E)\,. \tag{10}$$

Note that the transmission coefficient of (9) and (10) is exact.

*3.1.2 The Morse Barrier*

The Morse barrier is given by the expression

$$V_{\rm M}(r) = V_{\rm B}\left[2\,e^{-(r-R_{\rm B})/a_{\rm M}} - e^{-2\,(r-R_{\rm B})/a_{\rm M}}\right], \qquad (11)$$

where $R_{\rm B}$ and $V_{\rm B}$ are respectively the radius and the height of the barrier. Above, $a_{\rm M}$ is the Morse parameter, which is related to the second derivative of the potential at the barrier radius, $V''(R_{\rm B})$, by the expression,

$$a_{\rm M} = \sqrt{\frac{2\,V_{\rm B}}{-V''(R_{\rm B})}}.$$

This barrier has two convenient properties. The first is that it is asymmetric. Like the barriers of the total potential, it decreases rapidly on the left ($r < R_{\rm B}$) and slowly on the right ($r > R_{\rm B}$).

The second important property is that the transmission coefficient through a Morse barrier is known analytically. It is given by the expression [2]

$$T^{\rm M}(E) = \frac{1-\exp(-4\pi\alpha)}{1+\exp[2\pi\,(\beta-\alpha)]}, \qquad (12)$$

with

$$\alpha = k a_{\rm M} = \frac{\sqrt{2\mu E}}{\hbar}\,a_{\rm M} \quad \text{and} \quad \beta = \frac{\sqrt{2\mu V_{\rm B}}}{\hbar}\,a_{\rm M}. \qquad (13)$$

*3.1.3 Exact Barriers vs. Approximate Barriers*

The values of the parameters that fit the Coulomb barriers of the $^4$He + $^{16}$O, $^{12}$C + $^{16}$O, and $^{16}$O + $^{208}$Pb systems by parabolae and Morse functions are given in Table 2.

Figure 1 shows the Coulomb barriers (black solid lines) and the best fits by parabolae (blue dot-dashed lines) and by Morse functions (red dashed lines), for the three systems considered in this paper. The plots show the radial distances that influence the transmission coefficients at near-barrier energies. The figure leads to two conclusions. The first is that the fit by a Morse function is systematically better than by a parabola. This is not surprising, since the Morse function is asymmetric, as the Coulomb barrier itself, whereas the parabola is symmetric. The second conclusion is that the fits by the two functions are reasonable for $^{16}$O + $^{208}$Pb, but they are poor for the $^4$He + $^{16}$O and $^{12}$C + $^{16}$O systems. They become progressively worse as the system's mass decreases. The fits are particularly bad at $r \gg R_{\rm B}$, where the Coulomb potential decreases very slowly. Although the Morse function falls off more slowly on the external side of the barrier, it decreases exponentially, which is much faster than the $1/r$ decay of the Coulomb potential. As it will be shown in Section 4, the poor fits at large radial distances lead to dramatic overestimations of transmission coefficients and fusion cross sections at sub-barrier energies.

**Table 2** Parameters of the parabolic and of the Morse barriers that best fit the Coulomb barriers of the systems studied in the present paper

| System | $^4$He + $^{16}$O | $^{12}$C + $^{16}$O | $^{16}$O + $^{208}$Pb |
|---|---|---|---|
| $V_{\rm B}$ (MeV) | 2.90 | 7.99 | 76.55 |
| $R_{\rm B}$ (fm) | 7.42 | 8.02 | 11.59 |
| $\hbar\omega$ (fm) | 2.94 | 2.95 | 4.51 |
| $a_{\rm M}$ (fm) | 2.96 | 3.13 | 4.32 |

Note that the radius and the height of the barriers are the same for the two parametrizations. They differ only in the barrier curvature, given by $\hbar\omega$ and by $a_{\rm M}$ in the cases of the parabola and the Morse function, respectively

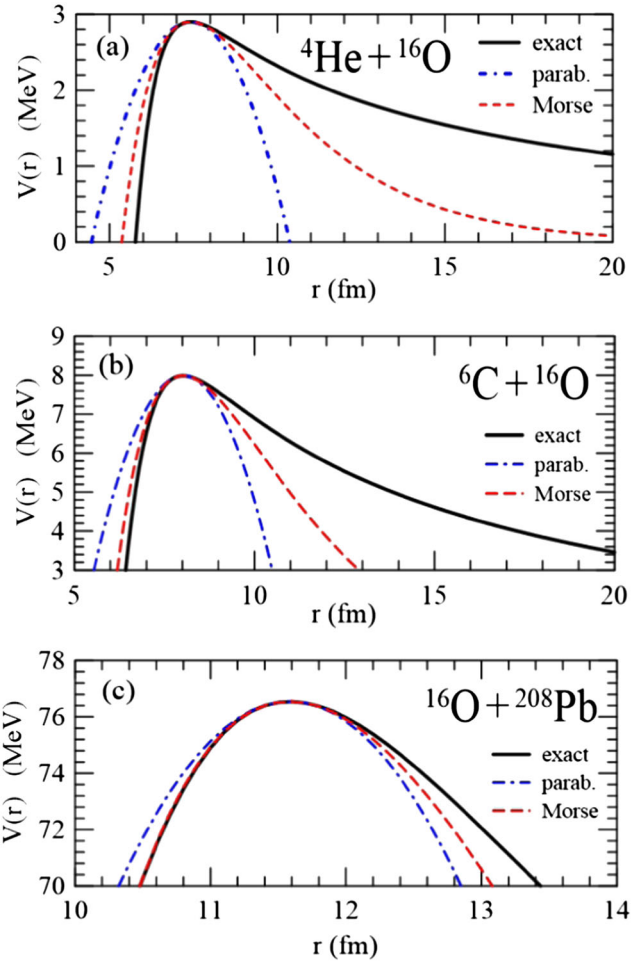


**Fig. 1** (Color on line) Fits of the Coulomb barrier (*black solid line*) by a parabola (*blue dot-dashed line*) and a Morse function (*red dashed line*). For details, see the text

### 3.2 WKB Transmission Coefficients

The WKB approximation is a short wavelength limit of quantum mechanics. Since it is extensively discussed in

textbooks on quantum mechanics and scattering theory [11, 14, 15], its derivation will not be presented here. We consider only the application of this approximation in calculations of transmission coeficients and fusion cross sections.

Let us consider a nucleus-nucleus collision at a sub-barrier energy $E$, with angular momentum $\hbar l$. Within the WKB approximation, the transmission coefficient is given by

$$T_l^{\rm WKB}(E) = \exp\left[-2\,\Phi^{\rm WKB}(E)\right], \tag{14}$$

where $\Phi^{\rm WKB}$ is the integral

$$\Phi^{\rm WKB}(E) = \int_{r_1}^{r_2} \kappa(r)\, dr, \tag{15}$$

with

$$\kappa(r) = \frac{\sqrt{2\mu\left[V_l(r) - E\right]}}{\hbar}. \tag{16}$$

In the above equations, $\mu$ is the reduced mass of the projectile-target system, $V_l(r)$ is the total potential of (1), and $r_1$ and $r_2$ are the classical turning points. They are the solutions of the equation on $r$,

$$V_l(r) = E. \tag{17}$$

The influence of multiple reflections under the barrier, ignored in the above equations, was investigated by Brink and Smilansky [16]. They concluded that these reflections are relevant at energies just below the barrier, contributing to improve the agreement with the exact results.

Although (14) is a very good approximation to the exact transmission coefficient at energies well below the barrier of the total potential, denoted by $B_l$, it becomes progressively worse as the energy approaches $B_l$. Furthermore, at energies above the barrier, the WKB transmission coefficient takes the constant value $T_l^{\rm WKB} = 1$, whereas its quantum mechanical counterpart is equal to 1/2 at the barrier and grows continually to one as the energy increases.

In 1935, Kemble [9] showed that the WKB approximation can be improved if one uses a better connection formula. He got the expression

$$T_l^{\rm K}(E) = \frac{1}{1 + \exp\left[2\,\Phi^{\rm WKB}(E)\right]}. \tag{18}$$

At energies well below the Coulomb barrier, the two turning points are far apart and $\kappa(r)$ reaches appreciable values within the integration limits of (15). In this way, $\Phi^{\rm WKB}(E)$ becomes very large, so that the unity can be neglected in the denominator of (18). This equation then reduces to (14). Therefore, the two approximations are equivalent in this energy region. However, Kemble's approximation remains valid as the energy approaches the barrier, leading to the correct result at $E = B_l$, namely $T_l = 1/2$.

### 3.3 Kemble Transmission Coefficient at Above-Barrier Energies

The problem with WKB approximations (both standard and Kemble's version) at above-barrier energies is that there are no classical turning points. At $E = V_{\rm B}$, the two turning points coalesce, and above this limit, (17) has no real solution. Then, $\Phi^{\rm WKB}\,(E > V_{\rm B}) = 0$, and the transmission coefficients of (14) and (18) take respectively the constant values $T_{\rm l}^{\rm WKB} = 1$ and $T_{\rm l}^{\rm K} = 1/2$.

However, Kemble [9] pointed out (see also the book by Fröman and Fröman [17], where this problem is treated formally) that (18) can be extended to above-barrier energies if one solves (17) in the complex r-plane and evaluates the integral between the complex turning points. Although Kemble [9] did not discuss this analytical continuation in detail, he pointed out that it would lead to the exact expression for the parabolic barrier below and above the barrier. More recently, the analytical continuation in the case of a typical heavy ion potential was carried out numerically [10], and the resulting transmission coefficient was shown to be in very good agreement with its quantum mechanical counterpart. In the next section, we carry out this analytical continuation in the cases of the parabolic and the morse barriers, where all calculations can be performed analytically.

#### *3.3.1 Transmission Through a Parabolic Barrier for $E > V_{\rm B}$*

Since the transmission coefficient through a parabolic barrier is known exactly, it is an ideal test for the analytical continuation procedure. However, before any consideration involving the complex plane, we prove that Kemble approximation for a parabolic barrier is exact at sub-barrier energies. For simplicity, we discuss in the section the particular case of a S-wave. The extension to other values of the angular momentum is straightforward. One has just to use the parameters of the $l$-dependent barrier, replacing $V_{\rm B} \to B_l$, $R_{\rm B} \to R_l$ and $\hbar\omega \to \hbar\omega_l$.

Since the exact transmission coefficient of (9) has the same general form of the Kemble transmission coefficient (18), the two expressions will be identical if

$$\Phi^{\rm WKB}(E) = \Phi^{\rm HW}(E). \tag{19}$$

Using the explicit forms of $\Phi^{\rm WKB}$ (15) and $\Phi^{\rm HW}$ (10), the above equation becomes,

$$\frac{\sqrt{2\mu}}{\hbar}\int_{r_-}^{r_+} dr\,\sqrt{V_{\rm B} - E - \frac{\mu\omega^2}{2}\,(r - R_{\rm B})^2} = \frac{\pi}{\hbar\omega}\,(V_{\rm B} - E)\,. \tag{20}$$

To calculate this integral, we make the transformation:

$$r \longrightarrow x = \omega\sqrt{\frac{\mu}{2}}\,(r - R_{\rm B})\,,$$

so that

$$dr = \frac{1}{\omega}\sqrt{\frac{2}{\mu}}\,dx, \quad r_{\pm} \to x_{\pm} = \pm\sqrt{V_{\rm B} - E}.$$

Equation (20) then becomes

$$\Phi^{\rm WKB} = \frac{2}{\hbar\omega}\int_{x_-}^{x_+} dx\,\sqrt{(V_{\rm B} - E) - x^2}. \tag{21}$$

This integral can be easily evaluated and the result is

$$\Phi^{\rm WKB} = \frac{\pi}{\hbar\omega}\,(V_{\rm B} - E)\,. \tag{22}$$

Thus, we conclude that Kemble approximation for a parabolic barrier is exact at sub-barrier energies.

Now, we consider collisions at above-barrier energies. To deal with this situation, we carry out the analytical continuation of $x$ to the complex plane. Setting $x \to z = x + i\,y$, the parabolic barrier becomes

$$V(z) = V_{\rm B} - z^2. \tag{23}$$

The turning points are then the complex solutions of the equation,

$$V(z) - E = 0, \tag{24}$$

for $E > V_{\rm B}$. Clearly, these turning points must be located on the complex r-plane, in a region where the potential is real. Solving (24) for a general potential is not simple. However, it can be easily done for a parabolic barrier, as that of (23). In this case, $V(z)$ is real only on the $x$ and on the $y$ axes. Therefore, the turning points must be either real or imaginary. The real turning points are the solutions of (24) for $E < V_{\rm B}$, which we have already discussed. Now, we consider the imaginary solutions. Inserting (23) into (24) and setting $z = iy$, one gets the coordinates of the two imaginary turning points,

$$y_{\pm} = \pm\sqrt{E - V_{\rm B}}.$$

Figure 2 shows a parabolic potential barrier (panel a) and its analytical continuation (panel b). The green circles on panel a, $x_-$ and $x_+$, represent the real turning points for an energy $E < V_{\rm B}$. The red circles in panel b, $y_-$ and $y_+$, indicate the imaginary turning points for an energy $E > V_{\rm B}$.

With the analytical continuation discussed above, the WKB integral of (21) can be extended to the complex plane. It must be evaluated along the imaginary axis, between the turning points $z_{\pm} = iy_{\pm}$. In this case, the integrand of (15) must be generalized as

$$\Phi^{\rm WKB} = \int_{r_-}^{r_+} \kappa(r)\,dr \;\to\; \Phi^{\rm WKB} = \int_{z_-}^{z_+} \kappa(z)\,dz. \tag{25}$$

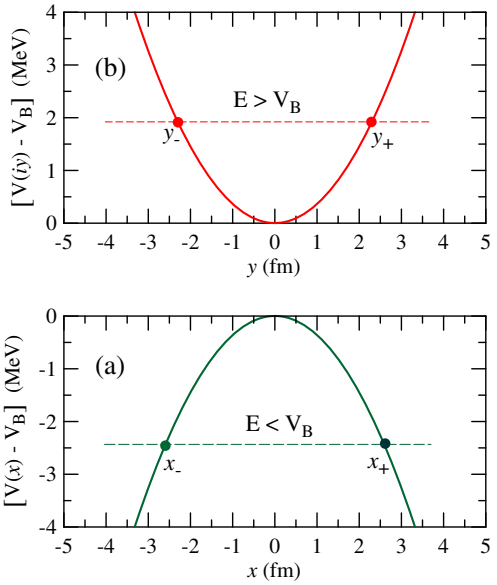


**Fig. 2** (Color on line) Analytical continuation of the parabolic potential barrier $V(x + iy)$. Panels **a** and **b** show respectively the potential on the real ($y = 0$) and on the imaginary ($x = 0$) axes. The figure also shows the real and the imaginary turning points in the cases of $E < V_{\rm B}$ (panel **a**) and $E > V_{\rm B}$ (panel **b**)

Using the explicit form of the potential (23) in (16) for $z = iy$, and changing the integration variable to $y$, one gets,

$$\Phi^{\rm WKB} = -\frac{2}{\hbar\omega}\int_{y_-}^{y_+} dy\,\sqrt{(E - V_{\rm B}) - y^2}.$$

This integral is equivalent to the one in (21), and the result is the same. Thus, we have shown that Kemble's formula for the transmission coefficient through a parabolic barrier is valid for any collision energy. Besides, it gives the exact quantum mechanical result.

### *3.3.2 Transmission Through a Morse Barrier for $E > V_{\rm B}$*

As in the previous section, we present a detailed discussion of the S-wave transmission coefficient. To extend it to other angular momenta, one has just to use the Morse parameter of the $l$-dependent barrier, changing $V_{\rm B} \to B_l$, $R_{\rm B} \to R_l$, and $a_{\rm M} \to a_l$.

We start with an important remark about the Morse approximation for the Coulomb barrier. In typical heavy ion collisions at near-barrier energies, the following relation is satisfied:

$$f(\mu, E) \equiv \exp(-4\pi\,\alpha) \equiv \exp\left(-\frac{4\pi\,a_{\rm M}\sqrt{2\mu E}}{\hbar}\right) \ll 1.$$

This term falls exponentially with the factor $\sqrt{\mu E}$. Thus, its largest values are for the lightest system, at the lowest collision energy. In the present study, it corresponds to $^4$He + $^{16}$O, at 0.5 MeV. Under these conditions, one gets $f(\mu, E) = 3 \times 10^{-5}$. For the other two systems, this term

is several orders of magnitude smaller. Therefore, it can be safely neglected, and (12) reduces to

$$T^{\mathrm{M}}(E) = \frac{1}{1+\exp\left[2\Phi^{\mathrm{M}}(E)\right]}. \tag{26}$$

Above,

$$\Phi^{\mathrm{M}}(E) = \pi\,(\beta-\alpha)\,, \tag{27}$$

where $\alpha$ and $\beta$ are given by (13). Comparing (26) and (18), one concludes that Kemble's approximation for the Morse barrier will be exact if the following condition is satisfied:

$$\Phi^{\mathrm{M}}(E) = \Phi^{\mathrm{WKB}}(E). \tag{28}$$

Using (15) and (27), the above condition becomes

$$\frac{\sqrt{2\mu}}{\hbar}\int_{r_-}^{r_+} dr\,\sqrt{V_{\mathrm{M}}(r)-E} = \pi\,(\beta-\alpha)\,, \tag{29}$$

where $r_\pm$ represents the solutions of the equation

$$V_{\mathrm{M}}\,(r_\pm) - E = 0.$$

These solutions can easily be determined and one finds

$$r_\pm = R_{\mathrm{B}} - a_{\mathrm{M}}\,\ln\left[1\pm\sqrt{1-\varepsilon}\right],$$

where we have introduced the notation

$$\varepsilon = \frac{E}{V_{\mathrm{B}}}.$$

To check the validity of (28), we evaluate the WKB integral of (29). Using the explicit form of the Morse potential (11) and changing to the new variable

$$r \;\longrightarrow\; t = \frac{\exp\left[-(r-R_{\mathrm{B}})/a_{\mathrm{M}}\right]-1}{\sqrt{1-\varepsilon}},$$

the integral takes the form

$$\Phi^{\mathrm{WKB}}(E) = \frac{\sqrt{2\mu V_{\mathrm{B}}}}{\hbar}\,a_{\mathrm{M}}\,(1-\varepsilon)\int_{-1}^{1} dt\,\frac{\sqrt{1-t^2}}{1+t\sqrt{1-\varepsilon}}.$$

This integral can be evaluated analytically and the result is

$$\Phi^{\mathrm{WKB}}(E) = \pi\,(\beta-\alpha)\,, \tag{30}$$

which coincides with the expression for $\Phi^{\mathrm{M}}(E)$ (27).

However, the above proof is not valid for $E > V_{\mathrm{B}}$. The reason is that $\Phi^{\mathrm{WKB}}$ was evaluated by an integration between two real turning points (see 29), which do not exist in this energy region. Nevertheless, the validity of (29) can be extended to $E > V_{\mathrm{B}}$, through an analytical continuation of the variable $r$. This procedure, which is analogous to the one adopted for a parabolic barrier, will be followed below.

First, we introduce the new projectile-target distance variable,

$$x = \frac{r-R_{\mathrm{B}}}{a_{\mathrm{M}}},$$

where the Morse parameter, $a_{\mathrm{M}}$, and the barrier radius, $R_{\mathrm{B}}$, are known quantities. Then, we perform the analytical continuation of $x$ to the complex plane. That is, $x \to z = x+i\,y$. Using the explicit expression of the potential in terms of $x$ and $y$, one gets

$$\begin{aligned} V(z) &= V_{\mathrm{B}}\,\left[2\,\exp\left(-x-iy\right)-\exp\left(-2x-2iy\right)\right] \\ &= U(x,y)+i\;W(x,y), \end{aligned}$$

with

$$U(x,y) = V_{\mathrm{B}}\left[2\,e^{-x}\,\cos y\,\left(1-e^{-x}\,\cos y\right)+e^{-2x}\right] \tag{31}$$

and

$$W(x,y) = 2\,V_{\mathrm{B}}\,e^{-x}\,\sin y\left[e^{-x}\,\cos y-1\right]. \tag{32}$$

Since, in the equation defining the turning points, the potential must be real, we set

$$W(x,y) = 0. \tag{33}$$

The solutions of the above equation are

$$\sin y = 0 \tag{34}$$

and

$$e^{x} = \cos y. \tag{35}$$

Equation (34) is satisfied on the real axis and on other horizontal lines intercepting the $y$ axis at $y = \pm n\pi$, where $n$ is any integer. It can be easily checked that the potential evaluated at any point on these lines cannot be higher than $V_{\mathrm{B}}$. Thus, there are no turning points on them. Therefore, these solutions must be discarded.

We are then left with the solutions of (35). They are curves on the complex plane confined to the left half-plane ($x < 0$). Similarly to (34), the periodicity of the trigonometric function (here $\cos y$) leads to an infinite number of solutions. They are curves that can be obtained from one another by shifts of $2\pi$ along the $y$ axis. Nevertheless, they lead to the same physics. Therefore, we concentrate on the one corresponding to the lowest values of $|y|$. This curve, denoted by $\Gamma$, is represented on panel a of Fig. (3). The turning points for $E = 2\,V_{\mathrm{B}}$ are represented by solid circles.

On the curve $\Gamma$, the variables $x$ and $y$ are not independent. They are related by (35). Thus, the potential becomes a function of a single variable. The coordinate $x$ along this curve is the single-valued function of $y$,

$$x_\Gamma(y) = \ln\left(\cos y\right). \tag{36}$$

Owing to the infinite values of the potential at $y = \pm\pi/2$, the coordinate $y$ is confined to the open interval $(-\pi/2, \pi/2)$. Then, $\cos y$ is positive, so that the solution of (36) is well defined.

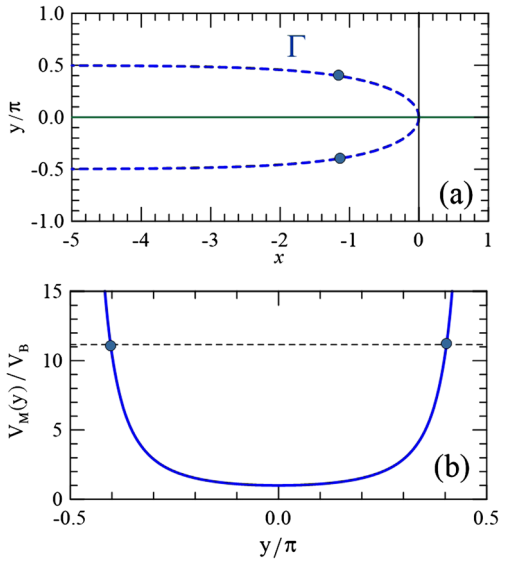


**Fig. 3** (Color on line) The analytic continuation of the Morse potential on the complex plane. Panel **a** shows the lines where the Morse potential is real. The *green solid line* is the trivial solution of (34) (the real axis), whereas the *blue dashed line*, labeled by Γ, is the solution of (35). The *solid circles* represent the turning points for an arbitrary energy above the barrier. Panel **b** shows the potential for points on Γ, where it is real, divided by $V_B$

To obtain the real potential for points on Γ, $U\,(x_\Gamma, y)$, one inserts (36) into (31). One gets,

$$U\,(x_\Gamma, y) \equiv U_\Gamma(y) = V_B\left[1 + \tan^2 y\right]. \tag{37}$$

Now, we evaluate the WKB integral on the complex plane,

$$\Phi^{\rm WKB}(E) = a_M\,\frac{\sqrt{2\mu}}{\hbar}\int_{z_-}^{z_+} dz\,\sqrt{V_M\,(z_\Gamma) - E}\,. \tag{38}$$

We remark that the factor $a$ results from the change of variable $r \to z = (r - R_B)/a_M$. For practical purposes, it is convenient to evaluate the integral over the contour Γ. On this contour, $V_M(x, y)$ reduces to the real potential of (37), $U_\Gamma(y)$, and the differential $dz$ can be written as

$$dz = \left[\frac{dx_\Gamma(y)}{dy} + i\right] dy,$$

where $dx_\Gamma(y)/dy$ is a real function of $y$. For energies above the barrier, $U_\Gamma(y) - E$ is negative so that,

$$\begin{aligned} dz\,\sqrt{U_\Gamma(y) - E} &= \left(\frac{dx_\Gamma(y)}{dy} + i\right) \times i\,\sqrt{E - U_\Gamma(y)}\,dy \\ &= G_R(y)\,dy + i\,G_I(y)\,dy, \end{aligned} \tag{39}$$

where $G_R(y)$ and $G_I(y)$ are the real functions,

$$G_R(y) = -\sqrt{E - U_\Gamma(y)}, \tag{40}$$

$$G_I(y) = \frac{x_\Gamma(y)}{dy}\,\sqrt{E - U_\Gamma(y)}. \tag{41}$$

The values of $y$ corresponding to the integration limits of (38) are given by the equation,

$$U_\Gamma(y) = E, \quad \text{or} \quad 1 + \tan^2 y = \varepsilon,$$

which has the solutions,

$$y_\pm = \pm\tan^{-1}\sqrt{1 - \varepsilon}.$$

Expressing the integral of (38) in terms of the variable $y$, one gets

$$\begin{aligned} \Phi^{\rm WKB}(E) = a_M\,\frac{\sqrt{2\mu}}{\hbar}\,&\int_{y_-}^{y_+} G_R(y)\,dy \\ &+ i\int_{y_-}^{y_+} G_I(y)\,dy\,. \end{aligned} \tag{42}$$

Inspecting Fig. 3, one concludes that $G_R(y)$ is an even function of $y$, whereas $G_I(y)$ is an odd function of $y$. Since the integration limits are symmetrical, the integration of $G_I(y)$ vanishes. Then, using the explicit form of $G_R(y)$ (40) with the potential of Eq. (37), one gets

$$\Phi^{\rm WKB}(E) = -a_M\,\frac{\sqrt{2\mu\,V_B}}{\hbar}\int_{y_-}^{y_+} dy\,\sqrt{(\varepsilon - 1)\,-\,\tan^2 y}\,. \tag{43}$$

To evaluate this integral, we change to the new variable, $y \to t = \tan y$, so the above integral becomes

$$\Phi^{\rm WKB}(E) = -a_M\,\frac{\sqrt{2\mu\,V_B}}{\hbar}\int_{-\sqrt{\varepsilon-1}}^{\sqrt{\varepsilon-1}} dt\,\frac{\sqrt{(\varepsilon - 1) - t^2}}{1 + t^2}\,. \tag{44}$$

The above integral can be found in standard integral tables, and the result is

$$\begin{aligned} \Phi^{\rm WKB}(E) &= \pi\,\frac{a_M\,\sqrt{2\mu V_B}}{\hbar}\left(1 - \sqrt{\varepsilon}\right) \\ &= \pi\,\left(\beta - \alpha\right). \end{aligned}$$

Thus, we have proved that Kemble's transmission coefficient through a Morse barrier reproduces accurately the exact quantum mechanical result, both below and above the Coulomb barrier.

### 3.4 Wong's Approximation for the Fusion Cross Section

In 1973, Wong [5] proposed a simple expression for the fusion cross section, in which the Coulomb barrier is approximated by a parabola, and the angular momentum is treated as a classical variable. Wong's formula is based on the following assumptions:

1. The fusion probability at the $l^{\rm th}$ partial wave is approximated by the Hill-Wheeler transmission factor

$$P_l^{\rm F}(E) \simeq \frac{1}{1 + \exp\left[2\pi\,(B_l - E)\,/\hbar\omega_l\right]},$$

with $B_l$ and $\hbar\omega_l$ standing for the height and the curvature parameters of the parabolic approximation for the barrier of $V_l(r)$.

2. The radii and the curvature parameters of the $l$-dependent barriers where assumed to be independent of $l$. That is $R_l = R_{l=0} \equiv R_B$ and $\hbar\omega_l = \hbar\omega_{l=0} \equiv \hbar\omega$. With this assumptions, the barrier height takes the simple form as follows:

$$B_l = V_B + \frac{\hbar^2\, l(l+1)}{2\mu\, R_B^2}. \tag{45}$$

.

3. The angular momentum is treated as the continuous variable $l \to \lambda = l + 1/2$. Then, one approximates the following: $l(l+1) \simeq \lambda^2$ and $\sum_l (2l+1) \to 2\int d\lambda\, \lambda$.

With these simplifying assumptions, (5) becomes

$$\sigma_F(E) = \frac{1}{E}\,\frac{\pi\hbar^2}{\mu}\int_0^\infty d\lambda\, \lambda\, T(\lambda, E),$$

where

$$T(\lambda, E) = \frac{1}{1 + \exp\left[\frac{2\pi}{\hbar\omega_l}\left(V_B - E + \frac{\hbar^2\lambda^2}{2\mu R_B^2}\right)\right]}.$$

The above integral can be evaluated analytically, and the result is Wong's cross section, which can be written as

$$\sigma_F^W(E) = R_B^2\,\frac{\hbar\omega}{2E}\,F_0(x). \tag{46}$$

Above, $x$ is the modified energy variable

$$x = \frac{E - V_B}{\hbar\omega}, \tag{47}$$

and $F_0(x)$ is the dimensionless and system-independent function

$$F_0(x) = \ln\left[1 + \exp(2\pi\, x)\right]. \tag{48}$$

This function is known in the literature as the *universal fusion function*. It is frequently used as a benchmark in comparative studies of fusion reactions [7, 18, 19].

#### *3.4.1 Energy Dependence of the Barrier Parameters*

Rowley and Hagino [20] pointed out that the barrier radius of $V_l(r)$ may decrease appreciably with $l$, mainly for light heavy ion systems. In this case, the radius for the grazing angular momentum may be a few fermi smaller that that for $l = 0$. Then, the approximation $R_l \simeq R_B$ is poor, and this makes Wong's formula inaccurate. The situation gets worse as the energy increases, so that $l_E$ takes large values. To cope with this situation, Rowley and Hagino proposed an improved version of the Wong formula, where the S-wave barrier parameters are replaced by the parameters associated with the grazing angular momentum.

The grazing angular momentum at the energy $E$, which we denote by $\lambda_E$, and the corresponding barrier radius, $R_E$, are given by the coupled equations as follows:

$$V_{\lambda_E}(r) = V_N(R_E) + V_C(R_E) + \frac{\hbar^2\,\lambda_E^2}{2\mu R_E^2} = E, \tag{49}$$

and

$$\left[\frac{dV_{\lambda_E}(r)}{dr}\right]_{R_E} = 0. \tag{50}$$

Solving these equations, one determines $l$E and $R$E, and the barrier curvature parameter is given by

$$\hbar\omega_E = \sqrt{\frac{-\hbar^2\, V''_{\lambda_E}(R_E)}{\mu}}.$$

The above equations supply the barrier parameters for the grazing angular momentum, which depends on the collision energy. Accordingly, the improved Wong formula becomes

$$\sigma_F^W(E) = R_E^2\,\frac{\hbar\omega_E}{2E}\,F_0(x_E), \tag{51}$$

where,

$$F_0(x_E) = \ln\left[1 + \exp(2\pi\, x_E)\right] \tag{52}$$

and

$$x_E = \frac{E - V_E}{\hbar\omega_E}. \tag{53}$$

Above, we have introduced the "effective Coulomb barrier" for the energy $E$,

$$V_E = B_\lambda - \frac{\hbar^2\,\lambda_E^2}{2\mu R_E^2} = V_N(R_E) + V_C(R_E). \tag{54}$$

The above expression is valid for $B_{\lambda_{crit}} \geq E \geq V_B$, where $\lambda_{crit}$ is the critical angular momentum, corresponding to the largest angular momentum where the total potential has a pocket. For energies below $V_B$, one sets $V_E = V_B$, $R_E = R_B$, and $\omega_E = \omega$. For energies above $B_{\lambda_{crit}}$, $V_E$ is given by (54) but with $B_\lambda$ replaced by $B_{\lambda_{crit}}$, and one sets $R_E = R_{\lambda_{crit}}$ and $\omega_E = \omega_{\lambda_{crit}}$.

## 4 Applications

Now, we discuss the use of the approximations of the previous sections to evaluate S-wave transmission coefficients and fusion cross sections. We perform calculations for a very light system and two slightly heavier ones, namely $^6$He + $^{16}$O, $^{12}$C + $^{16}$O, and $^{16}$O + $^{208}$Pb.

### 4.1 S-wave Transmission Coefficients

Figure 4 shows S-wave transmission coefficients obtained with the approximations discussed in the previous sections,

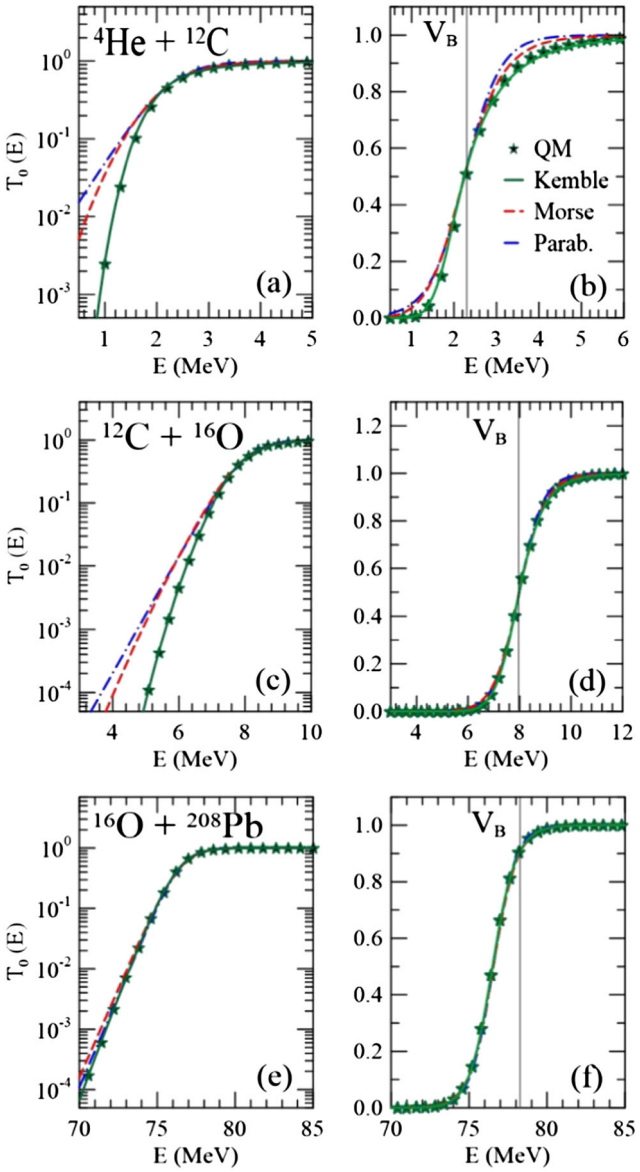


**Fig. 4** (Color on line) S-wave transmission coefficients for the $^4$He + $^{16}$O, $^{12}$C + $^{16}$O, and $^{16}$O + $^{208}$Pb at near-barrier energies. The figure shows the results for a parabolic barrier (*blue dot-dashed lines*) and for a Morse barrier (*red dashed lines*) and the predictions of Kemble's WKB approximation for the actual barrier (*green solid lines*), in comparison with the quantum mechanical results (*stars*). The results are shown in logarithmic (**a**, **c**, **e**) and linear (**b**, **d**, **f**) scales

in comparison with the exact quantum mechanical transmission coefficients (stars). The notation for the approximations are indicated in panel b. The results are shown in logarithmic scales (left panels), which is appropriate to compare cross sections at sub-barrier energies, and in linear scales (right panels), which gives a better picture at energies above the barrier. In the calculations of Kemble's transmission coefficients above the barrier, we used the elliptical approximation for the curves of real potential on the complex $r$-plane. As shown in Ref. [10], this approximation leads to accurate results, while it simplifies considerably the calculations.

In the case of the heaviest system, $^{16}$O + $^{208}$Pb, Kemble WKB (with the analytical continuation of $r$ [10]) reproduces the quantum mechanical transmission coefficient with great accuracy, above and below the Coulomb barrier. The other two curves, corresponding to approximations of the Coulomb barrier by a parabola (blue dot-dashed lines) and by a Morse function (red dashed lines) are very close to each other. They are also close to the exact results, except for the lowest energies in the plot, where the two approximations overestimate slightly the quantum mechanical results.

The situation is different for the $^4$He + $^{16}$O and $^{12}$C + $^{16}$O systems. Although Kemble's WKB remains very accurate, above and below the barrier, the parabolic and the Morse approximations are very poor at sub-barrier energies. These approximations greatly overestimate the transmission coefficients, by more than one order of magnitude at the lowest energies in the plots. In the case of the lightest system, $^4$He + $^{16}$O, the parabolic and the Morse approximations are also inaccurate at energies just above the barrier. It is clear that the results of the Morse approximation are systematically better than those of the parabola. Nevertheless, they are unsatisfactory, mainly at sub-barrier energies.

Figure 5 shows the fusion cross sections obtained with different approximations, in comparison with the exact cross sections (stars). The green solid lines are the results of Kemble WKB, the blue dot-dashed lines correspond to the Wong formula (46–48) and the red dashed lines correspond to the Morse approximation. That is, they are obtained evaluating the partial wave sum of (5), with $P_l^{\mathrm{F}}$ approximated by the transmission coefficient through the Morse barrier fitting $V_l(r)$.

The main trends of the fusion cross sections of the three systems are similar to the ones observed for the transmission coefficients. First, the Kemble WKB reproduces the exact results of the three systems with great accuracy, above and below the Coulomb barrier. Second, the Morse and the Wong cross sections for the $^{16}$O + $^{208}$Pb at sub-barrier energies reproduce the exact cross section fairly well. On the other hand, the cross sections of the $^4$He + $^{16}$O and $^{12}$C + $^{16}$O systems obtained with these approximations greatly overestimate the quantum mechanical cross section at sub-barrier energies. This is an immediate consequence of the abnormally large transmission coefficients of the parabolic and Morse barriers in this energy range.

On the other hand, one can observe an interesting trend of Wong's cross section at energies above the barrier. It is systematically larger than the quantum mechanical one. This discrepancy increases as the system's mass decreases. Rowley and Hagino [20] explained that this is a consequence of using a constant barrier radius, independent of the angular momentum. They pointed out that this problem

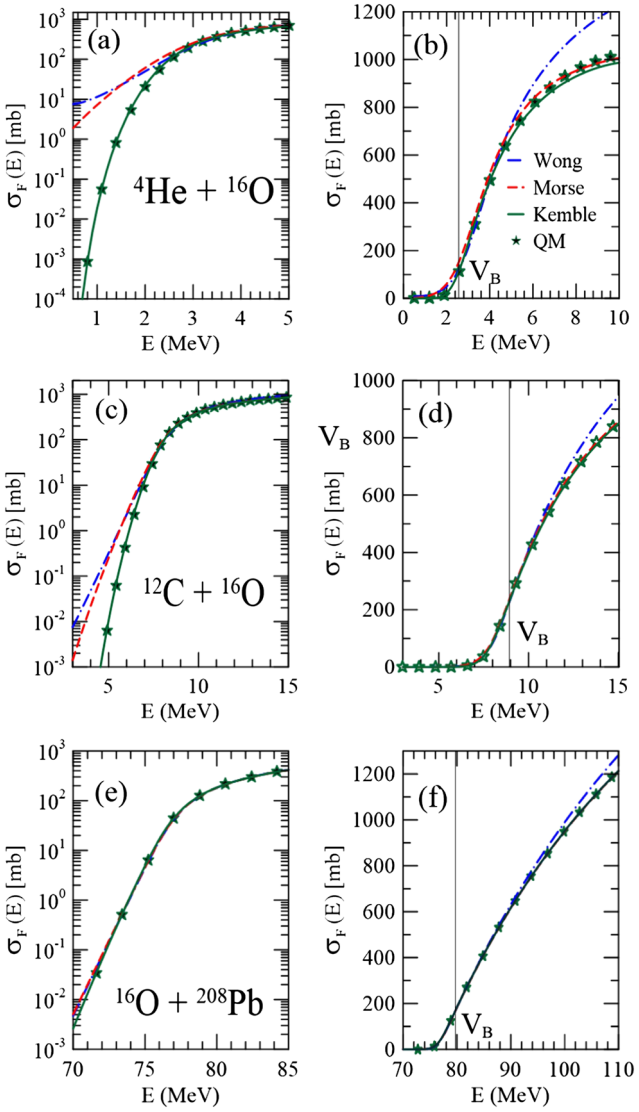


**Fig. 5** (Color on line) Fusion cross sections for the systems of the previous figures. The meaning of the *lines* are indicated within panel **b**

could be fixed by using the barrier parameters of the grazing angular momentum in Wong's formula, as described in Section 3.4.1. This is illustrated in Fig. 6, where we show the cross section obtained with the original Wong's formula (Wong 1) and the ones obtained with Wong's formula with energy-dependent parameters (Wong 2), as given by (51–53)). For comparison, we show also the corresponding quantum mechanical results (stars). For this illustration, we consider only the $^4$He + $^{16}$O system, where Wong's approximation above the barrier is worst. Since the two versions of the Wong formula are identical below the Coulomb barrier, it is not necessary to display the results in a logarithmic scale. Inspecting the figure, one concludes that the Wong formula with energy-dependent parameters of Ref. [20] works very well above the Coulomb barrier, even in the case of a very light system.

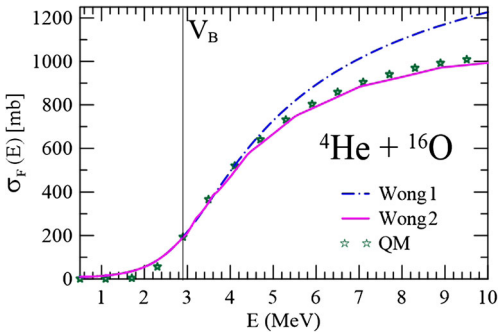


**Fig. 6** (Color on line) Fusion cross sections given by the original Wong formula (*Wong 1*) and by the improved Wong formula (*Wong 2*) for the $^4$He + $^{16}$O system, in comparison with the quantum mechanical results (*stars*)

## 5 Conclusions

We have studied the old problem of the one-dimensional tunneling in quantum scattering and fusion. First, we considered approximations of the barrier shape, by parabolae (Hill-Wheeler approximation) and by Morse functions. These approximations have the advantage of leading to analytical expressions for the tunneling probabilities. We investigated also the analytical continuation of the radial variable in Kemble's version of the WKB approximation for the parabolic and Morse barriers. We have shown that Kemble's WKB on the complex $r$-plane leads to exact transmission coefficients through these barriers and this conclusion is valid at energies below and above the barrier height.

Investigating the S-wave transmission coefficients for the $^4$He + $^{16}$O, $^{12}$C + $^{16}$O, and $^{16}$O + $^{208}$Pb systems, we found that the Morse barrier, being a more realistic non-symmetric function, leads systematically to better transmission coefficients. However, the improvement is not significative, as both approximations are poor at sub-barrier energies, except in the case of $^{16}$O + $^{208}$Pb, or heavier systems. On the other hand, the Kemble WKB approximation on the complex $r$-plane using the exact potential, developed in Ref. [10], gives a very accurate description of the quantum mechanical results, above and below the Coulomb barrier.

We performed calculations of fusion cross sections for the abovementioned systems using the Wong, the Morse, and Kemble WKB approximations. The conclusions were similar to the ones reached in the study of transmission coefficients. However, we found that the Wong formula overestimates the fusion cross section at energies above the barrier, mainly for very light systems. This shortcoming was then eliminated adopting the energy-dependent Wong formula of Rowley and Hagino [20].

**Acknowledgments** We are grateful to Raul Donangelo for critically reading the manuscript. Partial support from the Brazilian funding

agencies, CNPq, FAPESP, and FAPERJ, is acknowledged. M. S. H. acknowledges support from the CAPES/ITA Senior Visiting Professor Fellowship Program.

## References

1. K.W. Ford, D.L. Hill, M. Wakano, J.A. Wheeler, Ann. Phys. **7**, 239 (1959)
2. Z. Ahmed, Phys. Lett. A **157**, 1 (1991)
3. L.-L. Li, S.-G. Zhou, E.-G. Zhao, W. Scheid, Int. J. Mod. Phys. E **19**, 359 (2010)
4. D.L. Hill, J.A. Wheeler, Phys. Rev. **89**, 1102 (1953)
5. C.Y. Wong, Phys. Rev. Lett. **31**, 766 (1973)
6. L.F. Canto, P.R.S. Gomes, R. Donangelo, M.S. Hussein, Phys. Rep. **424**, 1 (2006)
7. L.F. Canto, P.R.S. Gomes, R. Donangelo, J. Lubian, M.S. Hussein, Phys. Rep. **596**, 1 (2015)
8. K. Hagino, N. Takigawa, Prog. Theor. Phys. **128**, 1061 (2012)
9. E.C. Kemble, Phys. Rev. **48**, 549 (1935)
10. A.J. Toubiana, L.F. Canto, M.S. Hussein, Eur. Phys. J. A **53**, 34 (2017)
11. L.F. Canto, M.S. Hussein, Scattering theory of molecules, atoms and nuclei. World Scientific Publishing Co. Pte. Ltd. (2013)
12. G.R. Satchler, W.G. Love, Phys. Rep. **55**, 183 (1979)
13. R.A. Broglia, A. Winther, Heavy ion reactions. Westview Press (2004)
14. E. Merzbacher, Quantum mechanics, 3rd ed. Wiley (1998)
15. C.J. Joachain, Quantum collision theory. North Holland (1983)
16. D.M. Brink, U. Smilansky, Nucl. Phys. A **405**, 301 (1983)
17. N. Fröman, P. Fröman, JWKB Approximation: contributions to the theory, 1st ed. North-Holland (1965)
18. L.F. Canto, P.R.S. Gomes, J. Lubian, L.C. Chamon, E. Crema, Nucl. Phys. A **821**, 51 (2009)
19. L.F. Canto, P.R.S. Gomes, J. Lubian, L.C. Chamon, E. Crema, J. Phys. G: Nucl. Part. Phys. **36**, 015109 (2009)
20. N. Rowley, K. Hagino, Phys. Rev. C **91**, 044617 (2015)